DALTON
FULL PAPER

# Ferromagnetic interactions and polymorphism in radical-substituted gold phosphine complexes

**Daniel B. Leznoff,[a] Corinne Rancurel,[a] Jean-Pascal Sutter,*[a] (the late) Steven J. Rettig,[b] Maren Pink,[c] Carley Paulsen[d] and Olivier Kahn*[a]**

[a] *Laboratoire des Sciences Moléculaires, Institut de Chimie de la Matière Condensée de Bordeaux, UPR CNRS No. 9048, F-33608 Pessac, France*
[b] *Department of Chemistry, University of British Columbia, 2036 Main Mall, Vancouver, B.C. V6T 1Z1, Canada*
[c] *X-Ray Crystallographic Center, Department of Chemistry, 160 Kolthoff Hall, University of Minnesota, Minneapolis, Minnesota 55455, USA*
[d] *Centre de Recherches sur les Très Basses Temperatures, UPR CNRS No. 5001, BP 166, F-38042 Grenoble, France*

***Received 23rd June 1999, Accepted 3rd September 1999***

A series of gold(I) complexes containing aminoxyl radical-substituted phosphine ligands has been prepared. Complexes chloro{2-[(*p*-diphenylphosphino)phenyl]-4,4,5,5-tetramethylimidazoline 1-oxyl 3-oxide}gold and [*tert*-butyl(*p*-diphenylphosphinophenyl)aminoxyl]chlorogold were prepared by reaction of the free radical phosphine with AuCl·THT (THT = tetrahydrothiophene) or by complexation of the radical precursor of the ligands to AuCl·THT followed by oxidation of the resulting gold complex. The first complex forms two distinct polymorphic crystal phases: in $CH_2Cl_2$–$Et_2O$ **2** crystallizes as green plates (α) in the triclinic space group $P\bar{1}$ and in $CH_2Cl_2$–hexanes as blue prisms (β) in the monoclinic space group $P2_1/a$. The crystal structures of both polymorphs and that of the complex **4** have been solved. The different solid-state arrangement of the molecules in the two polymorphic forms yields different magnetic behaviour; both exhibit intermolecular antiferromagnetic interactions but α exhibits a maximum in $\chi_m$ at 3.5 K while β shows no maximum. The favourable overlap of aminoxyl *N*-oxide groups in α causes this stronger interaction, which was modelled as a 1-D antiferromagnetic Heisenberg chain to give $J = -3.2$ cm$^{-1}$. The magnetic behaviour of the complex **4** was investigated down to 50 mK, showing dominant intermolecular ferromagnetic interactions but long range antiferromagnetic ordering at very low temperatures.

## Introduction

In the construction of metalloorganic radical systems, aminoxyl and alkylideneamine *N*-oxide radicals[1,2] have been widely used as ligands, both *via* their weakly basic N–O groups[3,4] and in conjunction with strong donor groups. The majority of such systems utilize hard nitrogen donors, especially planar N-heterocycles (*e.g.* pyridine, triazole), as co-ligands.[5–9] Such ligands have by their nature generally preferred complexation with hard metal centres. Phosphorus, the heavier congener of nitrogen, has a vast co-ordination chemistry of its own and yet phosphorus ligands have been notably absent in the synthesis of metalloorganic radical compounds. Phosphines offer several differences compared with more traditional nitrogen donors: their pseudo-tetrahedral geometry, their ability to co-ordinate soft, low-valent metal centres and finally access to the wealth of known co-ordination architectures involving phosphines.

Our recent synthesis of alkylideneamine *N*-oxide[10,11] and $^t$BuNO substituted triphenylphosphines[12] thus opens the door to the incorporation of soft, low-valent metal centres into molecular magnetic materials.[11] In particular we were attracted to $Au^I$ as a typical "soft" metal with a rich phosphine chemistry.[13,14] Gold(I), although diamagnetic, can act as an anchor in the construction of phosphine-containing molecules in which the spin carriers are located not at the metal centre but around the periphery. In addition, there are very few examples of gold being incorporated into molecular magnetic materials. A recent report of Gold(I) phosphine complexes in association with TCNE radical anions did not address their magnetic behaviour, although the structural chemistry was interesting.[15,16] Accordingly, analogues of [$Au(PPh_3)Cl$] using our novel paramagnetic phosphines have been synthesized and characterized. The series of compounds presented here are among the first molecule-based magnetic systems containing a soft gold centre and provide examples of polymorphism, antiferromagnetic and ferromagnetic interactions.

## Results and discussion

### Synthesis and characterization of gold phosphine-radical complexes

Reaction of the radical precursor **IH** with AuCl·THT[17] (THT = tetrahydrothiophene) in $CH_2Cl_2$ and subsequent *in situ* oxidation of the product **1** with $NaIO_4$ gave the final aminoxyl *N*-oxide gold phosphine complex **2** in good yield (Scheme 1). The same product could be obtained directly by reaction of AuCl·THT with phosphine **I** but in lower overall yield. Similarly, the reaction of *p*-$^t$BuNO$C_6H_4PPh_2$ **II** with AuCl·THT gave the corresponding gold phosphine complex **4** in high yield (Scheme 2). Ligation of the radical precursor **IIH** to the AuCl fragment to give **3**, followed by *in situ* oxidation with $Ag_2O$, was equally successful in producing the gold radical phosphine **4**. Note that although phosphine **II** rapidly decomposes in the solid state,[18] *in situ* co-ordination to the gold centre stabilizes the ligand, allowing for complexes to be isolated.

All of the complexes described are air- and moisture-stable systems and can be recrystallized from standard organic solvents. Complex **4** gives X-ray quality needles upon slow

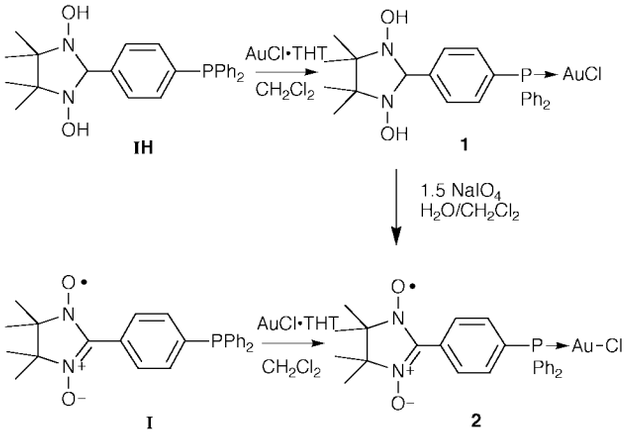


**Scheme 1**

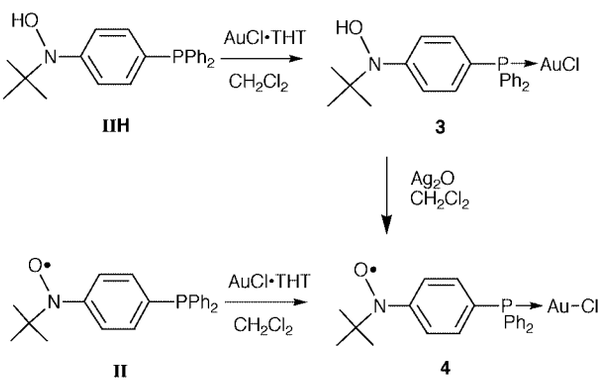


**Scheme 2**

evaporation of a $CH_2Cl_2$–hexanes solution. In the case of complex **2**, it was found that two crystal forms could be selectively crystallized, depending on the solvent mixture. A *green*, platelike polymorph, α-**2**, was produced by diffusion of diethyl-ether into a blue $CH_2Cl_2$ solution of **2**. Replacement of the diethyl ether with less polar hexanes as the diffusing solvent led to β-**2**, as dark *blue* block crystals. The elemental analysis indicated that the two sets of crystals did not contain solvent molecules; *i.e.* the presence or absence of solvent in the crystals did not play a role in the differences between the two isolated crystal forms. The infrared spectra of the two systems were substantially different. In particular, the diagnostic $\nu_{NO}$ vibration was found at 1364 $cm^{-1}$ for α-**2** and a strongly shifted 1355 $cm^{-1}$ for β-**2** (1368 $cm^{-1}$ for the "free" ligand **I**), indicating different solid-state structures were present. The ESR spectra of both complexes in solution gave the standard five-line pattern typical for aminoxyl *N*-oxide derivatives.[2] The solid-state UV-vis reflectance spectra of the two polymorphs both had one dominant broad band centred at 600 nm, that for α-**2** being slightly broader than that for β-**2**, hence accounting for the slight colour difference. Note that both crystal forms give identical blue solutions; colour differences are only observed in the solid state. No polymorphism is observed for the ᵗBuNO-substituted gold phosphine complex **4**. In order to probe the nature of the polymorphism of **2** and to understand the magnetic behaviour of the radical phosphine gold complexes (see below), X-ray crystallographic analyses were performed on α-**2**, β-**2** and **4**.

## Structural studies

**(a) α- and β-2 polymorphs.** Single crystals of complexes α- and β-**2** suitable for X-ray structural analysis were obtained as described above. The structural determination revealed that

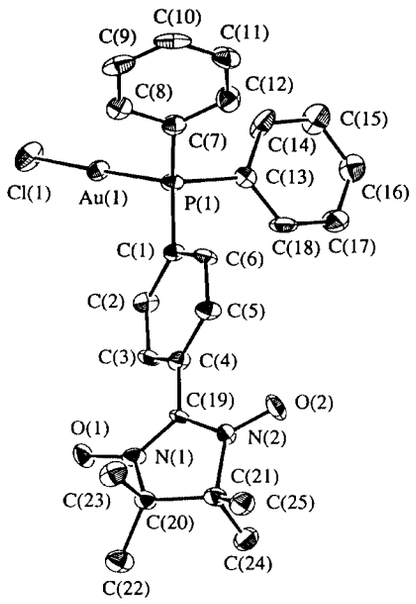


**Fig. 1** Molecular structure (ORTEP)[19] and numbering scheme for compound β-**2**, 33% ellipsoids. Selected bond lengths (Å) and angles (°) for β-**2** [α-**2**]: Au(1)–P(1) 2.2355(15) [2.235(2)]; Au(1)–Cl(1) 2.2971(15) [2.295(2)]; N(1)–O(1) 1.272(5) [1.278(9)]; N(2)–O(2) 1.257(5) [1.285(8)]; N(1)–C(19) 1.357(7) [1.347(10)]; N(2)–C(19) 1.363(6) [1.344(11)]; P(1)–Au(1)–Cl 174.43(6) [176.62(9)]. Bond lengths and angles are given for the Au(1)–containing molecule of α-**2**; values are similar for the other crystallographically independent molecule in the asymmetric unit of α-**2**.

the two crystal forms are true polymorphs, having exactly the same molecular connectivity and differ only in terms of crystal packing and minor conformational effects. The space groups are $P\bar{1}$ and $P2_1/a$ for α- and β-**2** respectively. Selected bond lengths and angles are in the caption of Fig. 1. In α-**2** there are two molecules in the asymmetric unit; they differ from one another by a slightly different conformational arrangement of the phenyl rings. There is only one molecule in the asymmetric unit of β-**2**. A view of the molecular structure of β-**2** is shown in Fig. 1 and is representative of those observed in α-**2** as well. The molecular structure of both compounds has the expected nearly linear geometry around the gold atom (P–Au–Cl is 176.62(9) and 172.30(9)° in α-**2** and 174.43(6)° in β-**2**). The Au–P bond lengths of 2.235(2) and 2.224(3) Å in the two independent molecules of α-**2** and 2.236(2) Å in β-**2** are comparable with the 2.235(3) Å found in $[Au(PP_3)Cl]$.[20] The Au–Cl distances are similarly unremarkable. The N–O bond lengths range from 1.257(5) to 1.287(9) Å as expected. Another parameter of interest, the dihedral angle between the aminoxyl *N*-oxide fragment and the phenyl ring to which it is bound, is approximately 30° in both α- and β-**2**; these are well within the values usually observed for phenyl-aminoxyl *N*-oxide species but significantly different from the coplanarity present in the closely related $Mo(CO)_5$ adduct of **I** recently reported.[11]

The differences between the two structures are to be found in the intermolecular crystal packing as opposed to the molecular structure. Polymorphism is a well studied phenomenon[21,22] and is especially relevant in magnetism; it is anticipated that polymorphs of open-shell complexes would have different magnetic behaviour as such behaviour is inherently a solid-state supramolecular effect.[23] Polymorphism in molecule-based magnetic systems is observed less frequently,[24] although the celebrated case of *p*-$NO_2$-phenyl-nitronyl nitroxide (the first organic ferromagnet) occurs in no less than four crystal phases, of which the β alone is a bulk ferromagnet.[25] In the case presented here, both α- and β-**2** exhibit roughly the same type of packing arrangement: a 2-D sheet of ligand fragments in the *ab* plane with the P–Au–Cl group filling the space between the

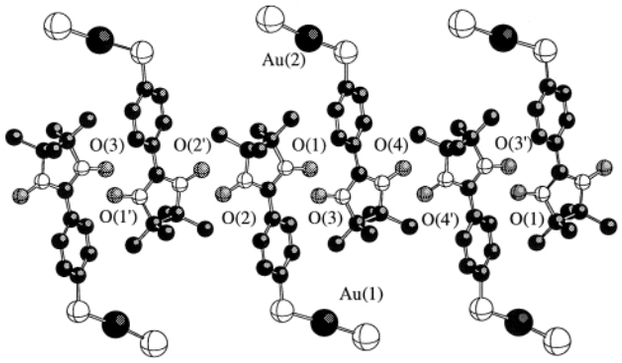


**Fig. 2** Projection of the structure of compound α-**2** on the *ac* plane (unsubstituted phenyl groups have been omitted for clarity). Selected intermolecular distances (Å): O(1)···N(3) 3.626; O(1)···O(3) 3.864; N(1)···O(3) 3.704; N(1)···N(3) 3.900; O(2)···N(2′) 3.693; O(2)···O(2′) 3.731; N(2)···N(2′) 4.081; O(4)···N(4′) 3.909; O(4)···O(4′) 4.052; N(4)···N(4′) 4.178.

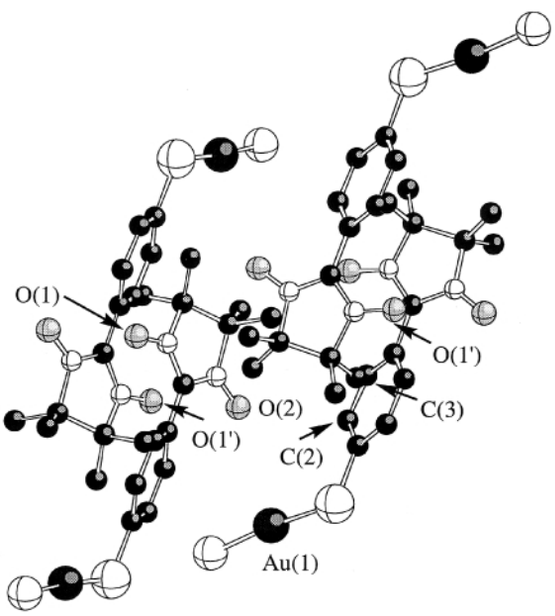


**Fig. 3** Projection of the structure of compound β-**2** on the *ac* plane (unsubstituted phenyl groups have been omitted for clarity). Selected intermolecular distances (Å): O(1)···O(1′) 3.909; O(1)···N(1′) 4.672; O(1)···C(3) 3.249; O(1)···H(2) 2.42; O(2)···C(2) 3.127; O(2)···Au(1) 3.456.

organic layers. In α-**2** the P–Au–Cl fragments orient in parallel with each other while in β-**2** they form a herringbone-like alternating arrangement along the *b* axis.

Important differences exist when examining intermolecular close contacts, particularly with respect to the radical-containing aminoxyl *N*-oxide fragments. A close intermolecular Au···O contact of 3.456(4) Å in the β phase is absent in α-**2**; this interaction manifests itself in the aforementioned large shift of $\nu_{NO}$ for β-**2** and in the slightly asymmetric N–O bond lengths (1.272(5) *vs*. 1.257(5) Å). The closest intermolecular contacts involving the aminoxyl O atoms in α-**2** are to the *meta* phenyl carbons (O(1)···C(2) 3.211; 2.55 Å to H) and *ortho*-phenyl carbons (O(1)···C(3), 3.265; 2.65 Å to H) of adjacent aminoxyl *N*-oxide groups. Similarly, for β-**2** the close contacts are O(1′)···C(3) (3.127; 2.81 Å to H) and O(2)···C(2) (3.249; 2.42 Å to H). More important, however, are the N–O/N–O interactions, which are substantially different in the two polymorphs. In α-**2**, three sets of N–O groups of adjacent aminoxyl *N*-oxide overlap (Fig. 2), forming nearly coparallel N(2)–O(2)/N(2′)–O(2′), N(1)–O(1)/N(3)–O(3) and N(4)–O(4)/N(4′)–O(4′) sets, with intermolecular distances from 3.693 to 4.081 Å in the first pair, 3.626 to 3.900 Å in the second and 3.909 to 4.178 Å

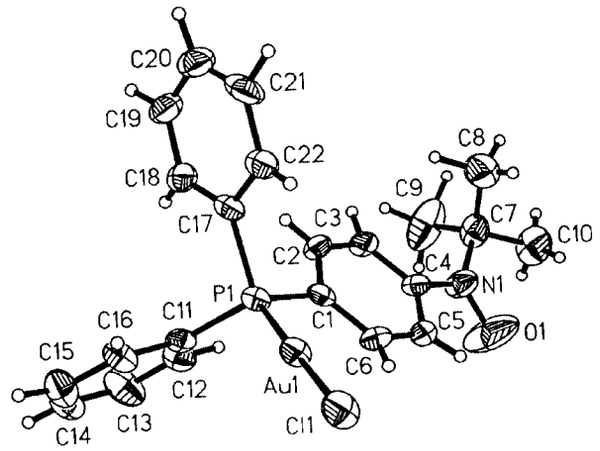


**Fig. 4** Molecular structure (ORTEP) and numbering scheme for compound **4**, 33% ellipsoids. Selected bond lengths (Å) and angles (°): Au(1)–P(1) 2.2294(14); Au(1)–Cl(1) 2.2860(14); N(1)–O(1) 1.274(6); P(1)–Au(1)–Cl(1) 177.77(6).

in the final pair respectively (see the caption of Fig. 2). The small range of intermolecular distances in the N–O/N–O paralellograms in α-**2** indicate a good overlap exists. On the other hand, in β-**2**, the intermolecular distances of O(1)···O(1′) (3.909 Å) and O(1)···N(1′) (4.672 Å) indicate a much less significant aminoxyl overlap and illustrate a different mode of packing (Fig. 3). Essentially the aminoxyl *N*-oxide groups form pseudo-chains within the *ab* plane aligned *ca*. 30° with respect to the *b* axis. Figs. 2 and 3 present views looking down the *b* axis along the chain length. As a result of these varied N–O interactions present in the two polymorphs, the magnetic behaviour of the two species is expected to be different.[26]

**(b) [Au(*p*-$^t$BuNOC$_6$H$_4$PPh$_2$)]Cl 4.** Compound **4** crystallizes in the space group $P2_12_12_1$. The crystal structure is shown in Fig. 4 (selected bond lengths and angles are in the caption) and reveals a molecule with similar geometric features to those of **2**. A linearly co-ordinated gold centre (P–Au–Cl angle is 177.77(6)°) is again observed, with Au–P and Au–Cl bond lengths of 2.229(2) and 2.286(2) Å respectively. The N–O bond length of 1.274(6) Å is comparable with those of other systems containing this fragment. The aminoxyl fragment lies 23.1(8)° out of the plane of the phenyl to which it is bound.

Compound **4** forms 2-D sheets in the *ab* plane, similar to that observed for **2** above. In this case the layers are in closer contact with each other; a O(1)···H–C(19) intermolecular contact of 2.496 Å exists, for example. This phenyl group does not have an appended radical moiety so the interplane contacts are likely magnetically unimportant. The key close intermolecular contacts involving the NO group are with the hydrogens of the adjacent $^t$BuNO moiety: O(1)···H–C(9) 2.850, O(1)···H–C(8) 3.148 and O(1)···H–C(10) 3.578 Å are all significant. This series of interactions generates 1-D chains of $^t$BuNO fragments within the *ab* plane that are effectively shielded from one another (Fig. 5).

Note that there are no close (<4 Å) intermolecular Au···Au contacts in any of the structures presented. Although aurophilic interactions are well known, it has been shown that bulky ligands inhibit their formation.[27] As [Au(PPh$_3$)Cl] itself does not exhibit aurophilic interactions, it is not surprising that these paramagnetic analogues are also devoid of Au···Au contacts. However, in general, the concept of using Au···Au interactions to create supramolecular magnetic architectures should be considered. The controlled assembly of a supramolecular lattice of individual molecules by hydrogen bond associations is a popular strategy in the design of molecular magnetic materials.[28–31] Gold–gold interactions, which are of equivalent

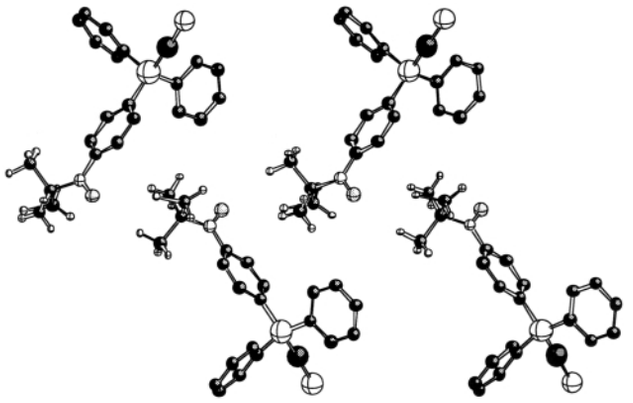

**Fig. 5** Projection of the structure of compound **4** on the *ab* plane. Phenyl hydrogens have been omitted for clarity. Selected intermolecular distances (Å): O(1)···H(9) 2.850; O(1)···H(8) 3.148; O(1)···H(10) 3.578; O(1)···C(8) 4.137; O(1)···C(9) 4.203.

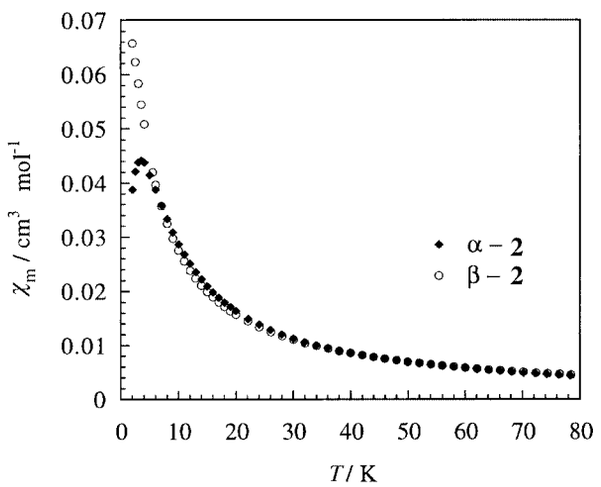


**Fig. 6** Temperature dependence of $\chi_M$ for compounds α- and β-**2**; a maximum in $\chi_m$ at 3.5 K for α-**2** is observable.

strength to weak hydrogen bonds,[32,33] could potentially be harnessed in a similar fashion.

## Magnetic properties

**(a) α- and β-2 polymorphs.** The temperature ($T$) dependences of the molar magnetic susceptibility ($\chi_m$) of compounds α- and β-**2** were measured in the range 2–300 K using an MPMS-5S SQUID susceptometer. At high temperatures $\chi_m T$ is 0.35 and 0.36 cm$^3$ K mol$^{-1}$ for α- and β-**2** respectively, as expected for non-correlated $S = 1/2$ spins. As the temperature is lowered to 2 K the $\chi_m T$ value of the compounds decreases to 0.08 and 0.13 cm$^3$ K mol$^{-1}$ respectively, consistent with intermolecular antiferromagnetic interactions. Upon examination of the $\chi_m$ *vs.* $T$ curves for the two polymorphs, shown in Fig. 6, however, more substantial differences can be observed. For α-**2** $\chi_m$ passes through a maximum at 3.5 K, after which it decreases. The curve for β-**2**, on the other hand, does not pass through any maximum to the limit of the experiment. It is clear that the antiferromagnetic interactions are substantially stronger in the α phase than in the β phase of **2**. The favourable overlap of the N–O groups (which contain high positive spin density[34]) in α-**2** provides a dominating mechanism for antiferromagnetic coupling, easily overwhelming the closer, yet intrinsically weaker N–O interaction with the *ortho* phenyl carbon (this interaction is assumed to be responsible for observed ferromagnetic interactions as in [Mo(CO)$_5$(**I**)][11]). In the case of β-**2** the N–O overlap is less efficient and hence the antiferromagnetic interactions are much weaker. The ESR of a polycrystalline sample of α-**2** at 10 K revealed a peak at half-field, consistent with a magnetically coupled system.

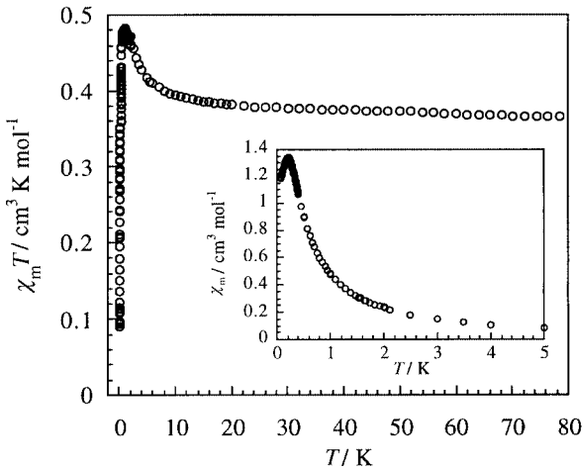


**Fig. 7** Temperature dependence of $\chi_m T$ for compound **4**. Inset: temperature dependence of $\chi_m$ between 50 mK and 5 K.

We have seen in the preceding section that the α-**2** phase from a magnetic point of view may be viewed as a 1-D system. The radical moieties, however, are not equally spaced along the chain direction, but show three slightly different interaction pathways, with O···O separations of 3.864, 3.731 and 4.052 Å successively. There is obviously no possibility to determine the various degrees of alternation, and as a first approximation the magnetic data were interpreted with a uniform 1-D model. The interaction parameter was then found as $J = -3.2$ cm$^{-1}$, with a spin Hamiltonian of the form $H = -JS_i \cdot S_{i+1}$.[35,36] It is worthwhile to note that, due to the alternation, the ground state may be considered as a singlet state, with a gap in the energy level spectrum between this singlet state and the first excited state. In the case of the β phase the complexity of the spin topology, together with the weakness of the interactions, encouraged us not to attempt to fit the magnetic data. Relevant examples for comparison include a zinc aminoxyl *N*-oxide chain complex (maximum in $\chi_m$ at 12 K) that was determined to be a 1-D antiferromagnet.[37] More spectacularly, several *N*-alkylpyridinium aminoxyl *N*-oxide compounds have been found to become diamagnetic at low temperatures due to the very strong coupling between proximate intermolecular N–O groups.[38–40] Similar behaviour was observed for pyrimidyl-[26] and imidazole-substituted[41] aminoxyls.

**(b) [Au(*p*-$^t$BuNOC$_6$H$_4$PPh$_2$)]Cl 4.** The temperature dependence of $\chi_m$ for a polycrystalline sample of compound **4** was measured in the temperature range 0.05–300 K. The plot of $\chi_m T$ *vs.* $T$ is shown in Fig. 7. At high temperature $\chi_m T$ is equal to 0.365 cm$^3$ K mol$^{-1}$, as expected for uncorrelated $S = 1/2$ spins and remains constant down to 60 K. As the temperature is lowered further $\chi_m T$ increases more and more rapidly, reaching a value of 0.49 cm$^3$ K mol$^{-1}$ at 1.0 K and decreases steeply as $T$ approaches absolute zero. In the linear part of the $1/\chi_m$ *vs.* $T$ graph (20–200 K) the magnetic susceptibility can be fitted with the Curie–Weiss law $\chi_m = 0.35/(T - 2.3)$. The behaviour depicted in Fig. 7 reveals the coexistence of dominant ferromagnetic and weaker antiferromagnetic interactions between the molecules along with a long-range antiferromagnetic ordering at a critical temperature, $T_N = 0.21$ K. The latter was determined as the temperature of the maximum of $\chi_m$.

It is likely that the key intermolecular interactions responsible for the ferromagnetic behaviour in compound **4** are the O(1)···H($X$) ($X$ = 8,9,10 of the adjacent $^t$Bu group) proximities, which generate a 1-D chain of NO···$^t$Bu groups. Taking into account a McConnell-type spin polarization mechanism,[42–44] the through-space magnetic interaction

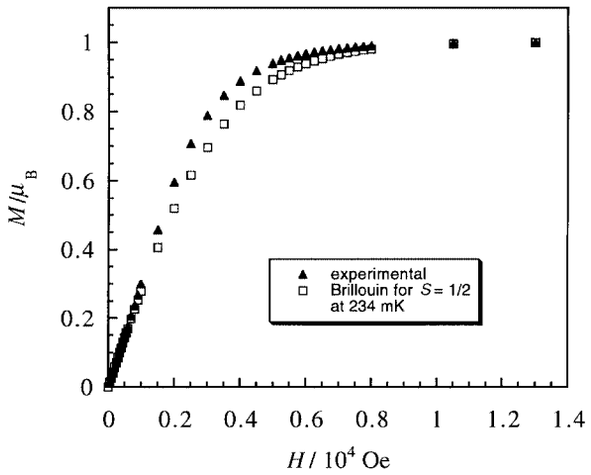


**Fig. 8** Field dependence of the magnetization for compound **4** at $T$ = 234 mK and the Brillouin curve for a spin $S$ = 1/2.

between the aminoxyl group, possessing positive spin density, and the ′Bu hydrogens (weak negative spin density)[34] should indeed lead to ferromagnetic behaviour. The antiferromagnetic ordering is most probably the result of weak antiferromagnetic interactions between these pseudo-chains. Using the high-temperature series expansion for a $S = 1/2$ one-dimensional ferromagnet, with a mean-field correction to account for the observed weak antiferromagnetic interactions, does not give physically reasonable interaction parameters. By this theoretical model, the ferromagnetic $J$ and the "weak" antiferromagnetic $zJ'$ are found to be of similar orders of magnitude, a result incompatible with the assumptions of the model.[45]

The field dependence of the magnetization was measured above $T_N$, at 234 mK. In Fig. 8 this magnetization curve is compared with the behaviour of isolated $S = 1/2$ spins at 234 mK calculated by the Brillouin function. As expected, the experimental curve shows a steep increase with the applied field to reach a saturation magnetization of *ca.* 1 $\mu_B$ within a field of 6000 Oe. At low fields the magnetization deviates upwards from the Brillouin curve, indicative of ferromagnetic interaction between the spin carriers. Reported intermolecular interactions between ′BuNO species tend to be antiferromagnetic in nature.[46–48] However, intermolecular ferromagnetic interactions in similar TEMPO (*N*-oxyl-tetramethylpiperidine)-type radicals have been described ($\theta$ values from +0.08 to +0.75 K have been reported)[49] and an example of a bulk ferromagnet based on a TEMPO species ($T_c = 0.18$ K, $\theta$ = 0.7 K) exists.[50]

## Conclusion

The synthesis of the first gold-containing molecular magnetic materials, based on radical-substituted triphenylphosphine, was accomplished. The use of gold(I) as a platform for arranging co-ordinated radicals in a linear geometry at the metal, and more generally the use of soft paramagnetic ligands with soft metals in molecular magnetic systems, was successfully illustrated. The observation of two gold–phosphine polymorphs with different magnetic properties serves to highlight the importance of crystal packing in molecular magnetism. The simple substitution of a aminoxyl *N*-oxide for a ′Bu aminoxyl group altered observed intermolecular antiferromagnetic interactions into ferromagnetic interactions in the solid state. This is the first crystal structure containing phosphine radical **II**; although the ligand was previously synthesized, it was found to be unstable in the solid state. Here, *in situ* co-ordination to a metal centre has stabilized the ligand, allowing for its use in magnetics studies. It can be noticed that the gold centre remains stable towards oxidation both in the presence of the paramagnetic phosphine ligand and in the oxidation step allowing a selective formation of the organic radical.

Finally, our attempts to increase the number of paramagnetic centres around the gold atom proved to be unsuccessful. Perhaps, a way to reach such polyradical species would be to use $Au^{III}$.

## Experimental

### General procedures

Unless otherwise stated all manipulations were performed in air using purified solvents. Silica gel (60A SDS, 70–200 μm) was used for separations as described below. The ESR spectra were recorded on a Bruker EMX instrument in $CH_2Cl_2$ solution at room temperature and in the solid state at 10 K, IR spectra using a Perkin-Elmer Paragon 1000 spectrometer and UV-vis reflectance spectra using a Cary 5E spectrophotometer. Microanalyses (C, H, N) were performed by the Centre National de la Recherche Scientifique (CNRS) central analysis service. The compound AuCl·THT[17] and phosphine ligands **I**[10,11] and **IIH**[12,18] were prepared by published procedures. Phosphine **IIH** was selectively oxidized at the N–OH group by $Ag_2O$ in $CH_2Cl_2$ at room temperature within fifteen minutes to give radical phosphine **II**, which was used *in situ*. All other reagents were obtained from commercial sources and used as received. Hexanes and $CH_2Cl_2$ were heated to reflux over $CaH_2$ under a nitrogen atmosphere and distilled prior to use; diethyl ether was distilled from sodium–benzophenone under a nitrogen atmosphere.

### Synthesis of compound 2 and recrystallization of polymorphs

Into a foil-protected round-bottomed flask was weighed AuCl·THT (0.068 g, 0.21 mmol). A solution of compound **IH** (0.089 g, 0.21 mmol) in 15 mL $CH_2Cl_2$ was added with stirring to the AuCl·THT, which rapidly dissolved to give a clear solution. This was stirred for 15 min, after which $NaIO_4$ (0.068 g, 0.32 mmol) dissolved in 10 mL water was added. The biphasic mixture was vigorously stirred for 15 min to give a dark green organic layer, which was separated, dried over $MgSO_4$ and evaporated to dryness *in vacuo* to give the product **2** as a green-blue powder. Yield: 0.11 g (80%). Recrystallization by slow diffusion of diethyl ether into a $CH_2Cl_2$ solution of crude **2** gave green plates of α-**2** suitable for structural analysis. Calc. for $C_{25}H_{26}AuClN_2O_2P$: C, 46.20; H, 4.03; N, 4.31. Found: C, 45.83; H, 4.23; N, 4.16%. IR (KBr): 1437, 1385, 1364 [$\nu$(NO)], 1301, 1217, 1167, 1135, 1103, 822 and 748 $cm^{-1}$. ESR ($CH_2Cl_2$, 298 K): 5-line pattern ($g = 2.006$; $a_N = 7.6$ G). UV-vis (reflectance, KBr): 600 nm. Recrystallization by slow diffusion of hexanes into a $CH_2Cl_2$ solution of crude **2** gave dark blue blocks of β-**2** suitable for structural analysis. Found: C, 45.42; H, 3.98; N, 4.25%. IR (KBr): 1436, 1385, 1355 [$\nu$(NO)], 1301, 1217, 1164, 1131, 1101, 832, 754 and 742 $cm^{-1}$. UV-vis (reflectance, KBr): 600 nm. Reaction of ligand **I** directly with AuCl·THT in $CH_2Cl_2$ (15 mL) gave **2** after 15 min of stirring and *in vacuo* removal of the solvent, but the difficulties involved in obtaining high yields of pure **I** obviate this route in favour of direct ligation of precursor **IH** to Au followed by oxidation as described above.

### Synthesis of [*tert*-butyl(*p*-diphenylphosphinophenyl)aminoxyl]-gold chloride 4

**Method A.** Phosphine **IIH** (0.050 g, 0.14 mmol) was dissolved in 15 mL $CH_2Cl_2$ in a foil-protected round-bottomed flask. To this was added $Ag_2O$ (0.033 g, 0.14 mmol) as a solid. Upon stirring for five minutes an orange colour developed and after 15 minutes the mixture was filtered through Celite directly onto solid AuCl·THT (0.046 g, 0.14 mmol) in another foil-protected

**Table 1** Summary of crystallographic data for compounds **2** and **4**

| | α-**2** | β-**2** | **4** |
|---|---|---|---|
| Formula | $C_{25}H_{26}AuClN_2O_2P$ | $C_{25}H_{26}AuClN_2O_2P$ | $C_{22}H_{23}AuClNOP$ |
| $M$ | 649.89 | 649.89 | 580.80 |
| Color, habit | Green, plate | Blue, prism | Tan, block |
| Crystal system | Triclinic | Monoclinic | Orthorhombic |
| Space group | $P\bar{1}$ | $P2_1/a$ | $P2_12_12_1$ |
| $a$/Å | 10.7694(8) | 13.8983(8) | 11.8932(2) |
| $b$/Å | 13.8406(13) | 11.2899(12) | 12.6364(2) |
| $c$/Å | 17.7718(8) | 15.4298(4) | 14.9445(2) |
| $\alpha$/° | 100.3860(5) | | |
| $\beta$/° | 91.9681(9) | 97.1748(5) | |
| $\gamma$/° | 109.926(2) | | |
| $V$/Å$^3$ | 2436.4(3) | 2402.1(2) | 2235.77(6) |
| Recorded reflections | 21939 | 21110 | 13537 |
| Observed reflections | | 6132 | 3936 |
| $Z$ | 4 | 4 | 4 |
| $D_c$/g cm$^{-3}$ | 1.772 | 1.797 | 1.725 |
| $\mu$/cm$^{-1}$ | 62.59 | 63.48 | 67.82 |
| $R$, $wR2$ | 0.0535, 0.055 | 0.037, 0.031 | 0.0263, 0.0413 |

flask. The AuCl·THT rapidly dissolved to give an orange solution, which was stirred for 15 min, after which the solvent was removed *in vacuo* to give a bright orange paste. This was redissolved in the minimum of $CH_2Cl_2$ and run through a short column of silica gel, the orange band being isolated. Removal of the solvent *in vacuo* gave an orange oil, to which was added 5 mL diethyl ether. Upon standing for several hours an orange microcrystalline powder of **4** was collected. Yield: 0.070 g (84%).

**Method B.** Into a foil-protected round-bottomed flask was weighed AuCl·THT (0.061 g, 0.19 mmol). A solution of **IIH** (0.065 g, 0.19 mmol) in 15 mL $CH_2Cl_2$ was added with stirring to AuCl·THT, which rapidly dissolved to give a clear solution. This was stirred for 30 min, after which $Ag_2O$ (0.043 g, 0.19 mmol) was added as a solid. The heterogeneous mixture was vigorously stirred and a yellow-orange solution rapidly formed. Stirring was continued for 30 min after which the mixture was filtered through Celite to give a bright orange solution. The solvents were removed *in vacuo* to give an orange solid which was redissolved in the minimum of $CH_2Cl_2$, purified by column chromatography and recrystallized as per Method A to give pure **4**. Yield: 0.081 g (74%). X-Ray quality needle crystals of **6** were obtained by slow evaporation of a $CH_2Cl_2$–hexanes solution. Anal. Calc. for $C_{22}H_{23}AuClNOP$: C, 45.49; H, 3.99; N, 2.41. Found: C, 45.20; H, 4.02; N, 2.54%. IR (KBr): 1479, 1435, 1407, 1368, 1239, 1185, 1102, 998, 842 and 831 cm$^{-1}$. ESR: 3-line pattern ($g$ = 2.005; $a_N$ = 11.9 G).

### Magnetic measurements

Magnetic susceptibility data were collected using a SQUID MSMS-5S magnetometer working down to 2 K at 1000 Oe field strength and a high-field low-temperature SQUID magnetometer developed at the Centre de Recherches sur les Très Basses Températures-CNRS. The latter is capable of measuring the magnetization at temperatures down to 50 mK. The data were corrected for the diamagnetism of the constituent atoms by use of Pascal constants.[45] Magnetization data were collected at 234 mK from 0.0–1.5 $T$ field strengths.

### X-Ray crystallographic analysis

**Compounds α- and β-2.** Crystallographic data appear in Table 1. Crystals were mounted on glass fibers and measured on a Rigaku/ADSC CCD diffractometer at 180(1) K. The data were processed and corrected for Lorentz-polarization effects and absorption.

The structures were solved by heavy-atom Patterson methods and expanded using Fourier techniques. There are two crystallographically independent molecules in the asymmetric unit of α-**2**. Full-matrix least-squares refinement was conducted with all non-hydrogen atoms anisotropic and hydrogen atoms in calculated positions.

**Compound 4.** Crystallographic data are in Table 1. A crystal was mounted on a glass fiber and measured on a Siemens SMART CCD system at 173(2) K. The data were processed using SAINT.[51] Final cell constants were obtained by performing a least-squares calculation on 8482 strong reflections. The data were corrected for absorption using SADABS.[51]

A direct-methods solution located most non-hydrogen atoms. The remaining atoms were found by conducting full-matrix least-squares and Fourier-difference cycles. All non-hydrogen atoms were refined with anisotropic displacement parameters and all hydrogen atoms with isotropic displacement parameters.

CCDC reference number 186/1639.

## Acknowledgements

This paper is dedicated to the memory of Steven J. Rettig, friend and colleague, who passed away suddenly on October 27, 1998. Financial support was provided by National Sciences and Engineering Research Council of Canada in the form of a Post-Doctoral Fellowship (to D.B.L.) and by the TMR Research Network ERBFMRXCT980181 of the European Union, entitled "Molecular Magnetism, from Materials toward Devices". The authors also thank Professors A. Laguna and M. Laguna (University of Zaragosa, Spain) for their valuable comments. The crystal structure of compound **4** was obtained at the X-ray Crystallography Laboratory, University of Minnesota in conjunction with Victor G. Young, Jr.

## References

1 J. H. Osiecki and E. F. Ullman, *J. Am. Chem. Soc.*, 1968, **90**, 1078.
2 E. F. Ullman, J. H. Osiecki, D. G. B. Boocock and R. Darcy, *J. Am. Chem. Soc.*, 1972, **94**, 7049.
3 A. Caneschi, D. Gatteschi, R. Sessoli and P. Rey, *Acc. Chem. Res.*, 1989, **22**, 392.
4 H. Iwamura, K. Inoue, N. Koga and T. Hayamizu, in *Magnetism: A Supramolecular Function*, ed. O. Kahn, Kluwer, Dordrecht, 1996.
5 K. Fegy, N. Sanz, D. Luneau, E. Belorizky and P. Rey, *Inorg. Chem.*, 1998, **37**, 4518.
6 F. A. Villamena, M. H. Dickman and D. R. Crist, *Inorg. Chem.*, 1998, **37**, 1454.
7 J.-P. Sutter, M. L. Kahn, S. Golhen, L. Ouahab and O. Kahn, *Chem. Eur. J.*, 1998, **4**, 571.
8 H. Oshio, T. Watanabe, A. Ohto and T. Ito, *Inorg. Chem.*, 1997, **36**, 1608.

9 S. Nakatsuji and H. Anzai, *J. Mater. Chem.*, 1997, **7**, 2161.
10 C. Rancurel, J.-P. Sutter, O. Kahn, P. Guionneau, G. Bravic and D. Chasseau, *New J. Chem.*, 1997, **21**, 275.
11 C. Rancurel, J.-P. Sutter, T. Le Hoerff, L. Ouahab and O. Kahn, *New J. Chem.*, 1998, **22**, 1333.
12 D. B. Leznoff, C. Rancurel, J.-P. Sutter, S. Golhen, L. Ouahab, S. J. Rettig and O. Kahn, *Mol. Cryst. Liq. Cryst.*, 1999, **334**, 425.
13 M. C. Gimeno and A. Laguna, *Chem. Rev.*, 1997, **97**, 511.
14 R. J. Puddephatt, in *Comprehensive Co-ordination Chemistry*, eds. G. Wilkinson, R. D. Gillard and J. A. McCleverty, Pergamon, Oxford, 1987, Vol. 5, p. 861.
15 E. Cerrada, M. C. Gimeno, A. Laguna, M. Laguna, V. Orera and P. G. Jones, *J. Organomet. Chem.*, 1996, **506**, 203.
16 P. J. Alonso, E. Cerrada, J. Garin, M. C. Gimeno, A. Laguna, M. Laguna and P. G. Jones, *Synth. Met.*, 1993, **55**–**57**, 1772.
17 R. Uson and A. Laguna, *Organomet. Synth.*, 1986, **3**, 322.
18 K. Torssell, *Tetrahedron*, 1977, **33**, 2287.
19 C. K. Johnson, ORTEP II, Report ORNL-5138, Oak Ridge National Laboratory, Oak Ridge, TN, 1976.
20 N. C. Baenziger, W. E. Bennett and D. M. Soboroff, *Acta Crystallogr., Sect. B*, 1976, **32**, 962.
21 J. Dunitz and J. Bernstein, *Acc. Chem. Res.*, 1995, **28**, 193.
22 D. Braga, F. Grepioni and G. R. Desiraju, *Chem. Rev.*, 1998, **98**, 1375.
23 *Magnetism: A Supramolecular Function*, ed. O. Kahn, Kluwer, Dordrecht, 1996.
24 J. S. Miller, *Adv. Mater.*, 1998, **10**, 1553.
25 M. Tamura, Y. Nakazawa, D. Shiomi, K. Nozawa, Y. Hosokoshi, M. Ishikawa, M. Takahashi and M. Kinoshita, *Chem. Phys. Lett.*, 1991, **186**, 401.
26 F. L. de Panthou, D. Luneau, J. Laugier and P. Rey, *J. Am. Chem. Soc.*, 1993, **115**, 9095.
27 M. Nakamoto, W. Hiller and H. Schmidbaur, *Chem. Ber.*, 1993, **126**, 605.
28 M. M. Matsushita, A. Izuoka, T. Sugawara, T. Kobayashi, N. Wada, N. Takeda and M. Ishikawa, *J. Am. Chem. Soc.*, 1997, **119**, 4369.
29 J. Veciana, J. Cirujeda, C. Rovira, E. Molins and J. J. Novoa, *J. Phys. I. Fr.*, 1996, **6**, 1967.
30 A. Lang, Y. Pei, L. Ouahab and O. Kahn, *Adv. Mater.*, 1996, **8**, 60.
31 N. Yoshioka, M. Irisawa, Y. Mochizuki, T. Kato, H. Inoue and S. Ohba, *Chem. Lett.*, 1997, 251.
32 H. Schmidbaur, *Chem. Soc. Rev.*, 1995, 391.
33 D. M. P. Mingos, *J. Chem. Soc.*, *Dalton Trans.*, 1996, 561.
34 A. Zheludev, V. Barone, M. Bonnet, B. Delley, A. Grand, E. Ressouche, P. Rey, R. Subra and J. Schweizer, *J. Am. Chem. Soc.*, 1994, **116**, 2019.
35 J. C. Bonner and M. E. Fisher, *Phys. Rev. A*, 1964, **135**, 646.
36 J. W. Hall, W. E. Marsh, R. R. Weller and W. E. Hatfield, *Inorg. Chem.*, 1981, **20**, 1033.
37 A. Caneschi, D. Gatteschi, R. Sessoli, C. I. Cabello, P. Rey, A. L. Barra and L. C. Brunel, *Inorg. Chem.*, 1991, **30**, 1882.
38 K. Ueda, M. Tsujii, T. Suga, T. Sugimoto, N. Kanehisa, Y. Kai and N. Hosoito, *Chem. Phys. Lett.*, 1996, **253**, 355.
39 K. Awaga, A. Yamaguchi and T. Oki, *Mol. Cryst. Liq. Cryst.*, 1995, **271**, 97.
40 K. Awaga, T. Inabe, U. Nagashima, T. Nakamura, M. Matsumoto, Y. Kawabata and Y. Maruyama, *Chem. Lett.*, 1991, 1777.
41 R. Akabane, M. Tanaka, K. Matsuo, N. Koga, K. Matsuda and H. Iwamura, *J. Org. Chem.*, 1997, **62**, 8854.
42 H. M. McConnell, *J. Chem. Phys.*, 1963, **39**, 1910.
43 H. Iwamura, *Adv. Phys. Org. Chem.*, 1990, **26**, 179.
44 D. A. Dougherty, *Acc. Chem. Res.*, 1990, **24**, 88.
45 O. Kahn, *Molecular Magnetism*, VCH, Weinheim, 1993.
46 M. Kitano, Y. Ishimaru, K. Inoue, N. Koga and H. Iwamura, *Inorg. Chem.*, 1994, **33**, 6012.
47 Y. Ishimaru, M. Kitano, H. Kumada, N. Koga and H. Iwamura, *Inorg. Chem.*, 1998, **37**, 2273.
48 T. Ishida and H. Iwamura, *J. Am. Chem. Soc.*, 1991, **113**, 4238.
49 K. Togashi, R. Imachi, K. Tomioka, H. Tsuboi, T. Ishida, T. Nogami, N. Takeda and M. Ishikawa, *Bull. Chem. Soc. Jpn.*, 1996, **69**, 2821.
50 T. Nogami, K. Tomioka, T. Ishida, H. Yoshikawa, M. Yasui, F. Iwasaki, H. Iwamura, N. Takeda and M. Ishikawa, *Chem. Lett.*, 1994, 29.
51 SAINT, Siemens Industrial Automation, Inc., Madison, WI, 1999; G. M. Sheldrick, SADABS, Program for Siemens area detector absorption correction, Institut für Anorganische Chemie, Universität Göttingen, 1996.

*Paper 9/05026D*